JBC ARTICLE

The intermembrane space protein Mix23 is a novel stress-induced mitochondrial import factor

Received for publication, May 6, 2020, and in revised form, August 19, 2020 Published, Papers in Press, August 21, 2020, DOI 10.1074/jbc.RA120.014247

Eva Zöller[1,‡], Janina Laborenz[1,‡], Lena Krämer[1], Felix Boos[1], Markus Räschle[2], R. Todd Alexander[3], and Johannes M. Herrmann[1,*]

From the Departments of [1]Cell Biology and [2]Molecular Genetics, University of Kaiserslautern, Kaiserslautern, Germany and the [3]Department of Pediatrics, University of Alberta, Edmonton, Alberta, Canada

Edited by Ursula Jakob

The biogenesis of mitochondria requires the import of hundreds of precursor proteins. These proteins are transported post-translationally with the help of chaperones, meaning that the overproduction of mitochondrial proteins or the limited availability of chaperones can lead to the accumulation of cytosolic precursor proteins. This imposes a severe challenge to cytosolic proteostasis and triggers a specific transcription program called the mitoprotein-induced stress response, which activates the proteasome system. This coincides with the repression of mitochondrial proteins, including many proteins of the intermembrane space. In contrast, herein we report that the so-far-uncharacterized intermembrane space protein Mix23 is considerably up-regulated when mitochondrial import is perturbed. Mix23 is evolutionarily conserved and a homolog of the human protein CCDC58. We found that, like the subunits of the proteasome, Mix23 is under control of the transcription factor Rpn4. It is imported into mitochondria by the mitochondrial disulfide relay. Mix23 is critical for the efficient import of proteins into the mitochondrial matrix, particularly if the function of the translocase of the inner membrane 23 is compromised such as in temperature-sensitive mutants of Tim17. Our observations identify Mix23 as a novel regulator or stabilizer of the mitochondrial protein import machinery that is specifically up-regulated upon mitoprotein-induced stress conditions.

Mitochondrial biogenesis relies on the import of hundreds of protein precursors from the cytosol. Proteins of the mitochondrial matrix are synthesized with N-terminal presequences or matrix targeting signals (MTSs) which bind to surface receptors on the mitochondrial outer membrane (1, 2). These receptors are associated with the translocase of the outer mitochondrial membrane (TOM) complex, which serves as a general entry gate for protein import (3–6). After translocation through the protein-conducting channel in the TOM complex, MTSs engage with the TIM23 complex of the inner membrane, which facilitates their further transport into the matrix via a reaction driven by the inner membrane potential and by Hsp70-mediated ATP hydrolysis (7, 8). The interactions between the TOM and TIM23 complex are dynamically regulated by the incoming preproteins and depend on intermembrane space (IMS)-exposed protein domains of several proteins, including Tom22, Tim50, Tim21, and Tim23 (9–13).

Most IMS proteins lack MTSs and employ a unique import mechanism independent of ATP and the inner membrane potential (14–16). Many of these IMS proteins contain characteristic cysteine residues that are part of their targeting signal (17, 18). These mitochondrial IMS sorting signal or IMS targeting signal sequences direct proteins through the protein-translocation pore of the TOM complex into the IMS, where they associate with the hydrophobic substrate-binding region of Mia40 (19, 20). Mitochondrial intermembrane space import and assembly protein 40 (Mia40; coiled-coil-helix-coiled-coil-helix domain containing 4 (CHCHD4) in humans) contributes at least two functions: 1) it traps incoming IMS precursors via a hydrophobic interaction with their mitochondrial IMS sorting signal/IMS targeting signal and 2) it introduces disulfide bonds into these substrates (21–23).

Most Mia40 substrates share a simple helix-loop-helix structure in which both helices are stabilized by two parallel disulfide bonds (24–27). Because of the specific spacing of the cysteine residues in their primary sequence, these proteins are referred to as twin Cx_3C or twin Cx_9C proteins. However, some Mia40 substrates show different numbers and arrangements of their cysteine residues: whereas Mia40 introduces five disulfides into the IMS protease Atp23, it is critical for the formation of a single disulfide bond in the inner membrane proteins Tim17 and Tim22 (28–31).

The protein import into mitochondria is under surveillance of the proteasome. Arrested mitochondrial import intermediates induce severe stress, presumably because of the accumulation of non-imported mitochondrial precursor proteins in the cytosol (32–37). Conditions that perturb mitochondrial import trigger a characteristic stress response that leads to an induction in expression of many chaperones and the constituents of the proteasome (Fig. 1*A*) (33, 34, 38). Here we identify the poorly characterized protein Mix23 as one of few IMS proteins that are induced under these stress conditions. Mix23 is critical for efficient protein import into mitochondria, and deletion of Mix23 in temperature-sensitive *tim17* mutants leads to synthetic defects in growth and the import of proteins into the mitochondrial matrix. Our results suggest that Mix23 is a stress-regulated factor that is relevant for efficient protein translocation into mitochondria.

This article contains supporting information.
[‡]These authors contributed equally to this work.
*For correspondence: Johannes M. Herrmann, hannes.herrmann@biologie.uni-kl.de.

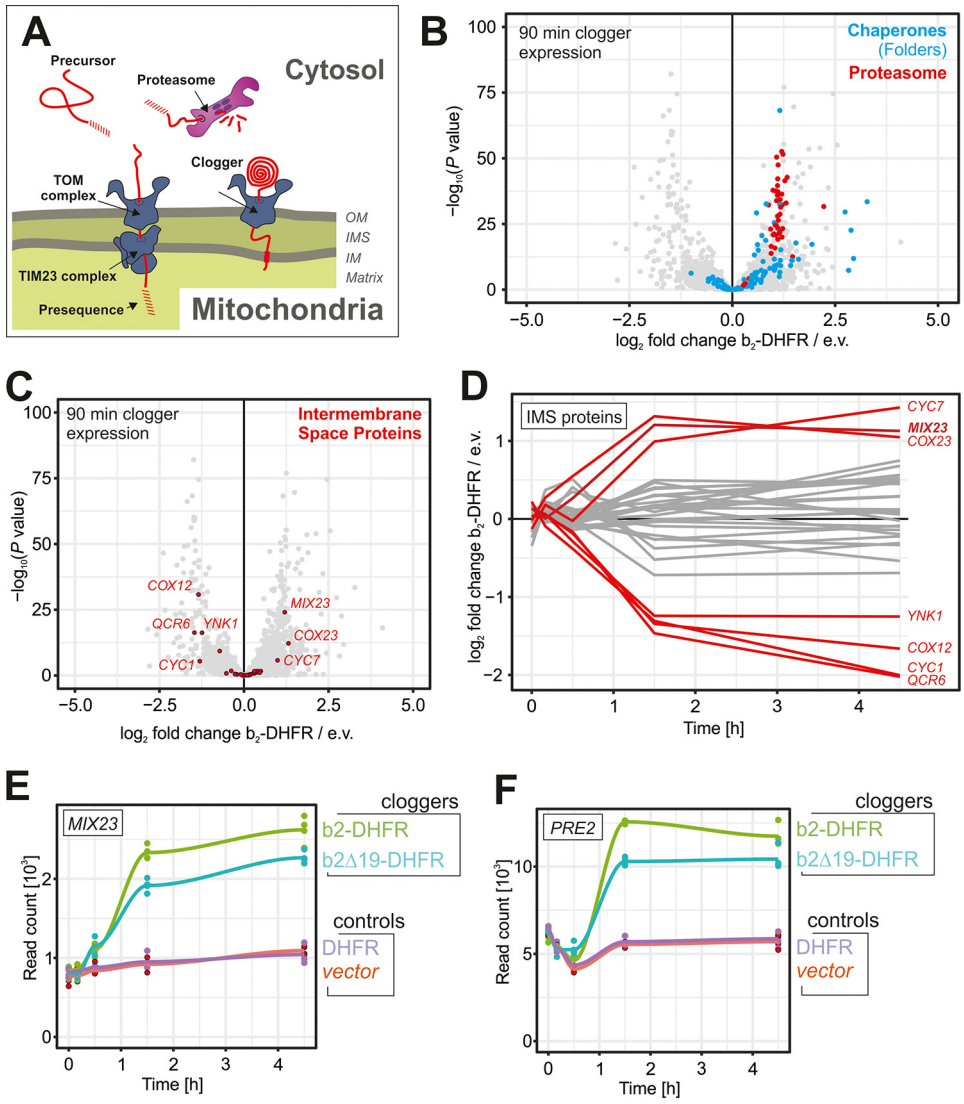

Figure 1. The expression of clogger induces *MIX23* expression. *A*, schematic representation of the mitochondrial import machinery and the cytochrome b_2-DHFR construct (Clogger) (33). *B*, cells expressing the clogger construct or an empty vector for control were shifted for 90 min from lactate medium to lactate + 0.5% galactose medium. Cellular mRNA was isolated from three biological replicates and sequenced (33). Many chaperone (*blue*) and proteasome subunit (*red*) genes were induced by clogger expression. *C*, most IMS proteins (*red*) were not significantly increased upon mitoprotein-induced stress. However, clogger expression leads to an up-regulation of Mix23. *D*, shown are the relative changes in clogger *versus* control expression of genes coding for IMS proteins (39). Dually localized proteins that are predominantly located in the cytosol were omitted. *E* and *F*, RNA levels of *MIX23* and *PRE2* (coding for a proteasome subunit) are shown for different times after clogger induction. See (33) for details.

Results

Stalled import intermediates selectively induce Mix23 expression

Cloggers are slowly imported mitochondrial precursor proteins that competitively inhibit mitochondrial translocation *in vivo* and activate the mitoprotein-induced stress response. Because of their slow import, inner membrane proteins with N-terminal stop-anchor sequences (also called bipartite presequences) have particularly strong competitive effects (32, 33). These proteins include model substrates such as cytochrome b_2-DHFR and endogenous inner membrane proteins such as cytochrome c oxidase 11 (Cox11) or Cox5a. To assess the effect of clogger expression on proteins of the mitochondrial IMS, we analyzed the data from our previous study (33) in which the cellular mRNA levels were followed after induction of the model protein cytochrome b_2-DHFR for 90 min compared with control cells, which did not express the clogger protein. Whereas most chaperones and proteasome subunits were up-regulated under these conditions (Fig. 1*B*), the reaction of the gene expression of IMS proteins was more heterogeneous (Fig. 1, *C* and *D*). However, three IMS proteins, Mix23, cytochrome c 7 (Cyc7), and Cox23, were considerably up-regulated by expression of cytochrome b_2-DHFR. Mix23 (initially named Mic23 but then renamed to avoid confusion with mitochondrial contact site and cristae organizing system (MICOS) components) is a poorly characterized protein with unknown function (39, 40). Its up-regulation followed a similar kinetics as that of proteasome subunits (compare Fig. 1, *E* and *F*) and was also observed with matrix-targeted proteins such as cytochrome $b_2\Delta_{19}$-DHFR. This indicates that the mitoprotein-induced stress response leads to the induction of Mix23.

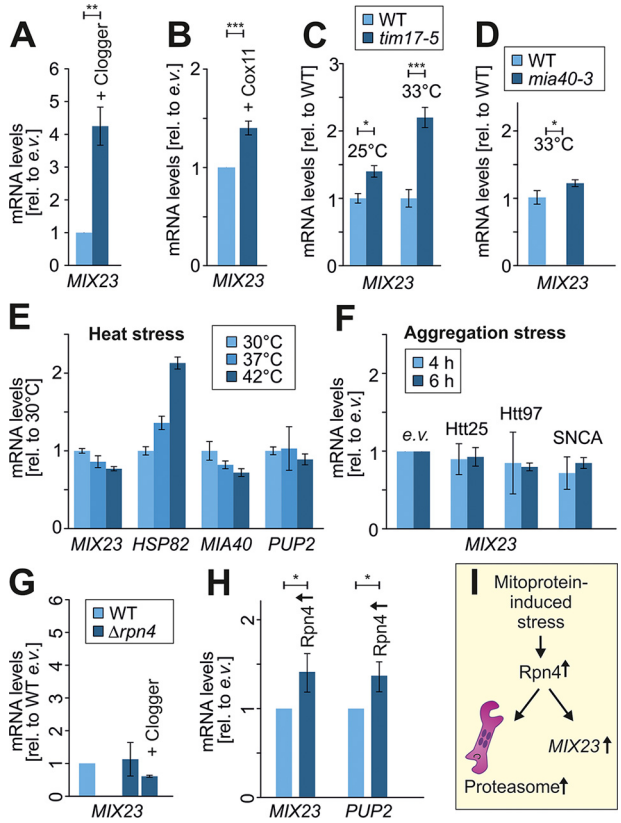

Figure 2. Mitoprotein-induced stress conditions specifically increase *MIX23* expression. *A*, WT cells with empty vector (*e.v.*) or *GAL1*-driven cytochrome b_2-DHFR plasmid (Clogger) were shifted to galactose-containing lactate medium for 4 h. RNA was isolated and *MIX23* mRNA levels (and controls) were quantified by qPCR. The values shown were normalized as described under "Experimental procedures." Mean values of six (three biological and three technical) replicates are shown and were used for a Student's *t* test. $*p < 0.05$, $**p < 0.01$, $***p < 0.005$. *B*, the experiment was repeated as in (*A*) but *GAL-COX11* was used instead of the clogger plasmid. *C and D*, *MIX23* expression was analyzed in WT, *tim17-5*, and *mia40-3* cells at permissive (25 °C) growth conditions and after a 24-h shift to semi-restrictive (33 °C) conditions. *E*, WT cells were grown in galactose medium and shifted for 2 h to the indicated temperatures. *F*, WT cells were transformed with plasmids for expression of Htt25-GFP, Htt97-GFP, or α-synuclein (*SNCA*), or with an empty vector for control. After the shift to galactose for 4 or 6 h, *MIX23* RNA levels were quantified. *G*, *MIX23* levels were measured in Δ*rpn4* cells as described in (*A*). Values were normalized to WT levels. *H*, Rpn4 was overexpressed from a multicopy plasmid under control of the constitutive *CYC1*-promoter (49). *I*, mitoprotein-induced stress leads to the simultaneous induction of *MIX23* and the proteasome in an Rpn4-dependent manner.

Mix23 is up-regulated upon mitoprotein-induced stress but not upon heat stress

Next, we performed real-time qPCR measurements to study the expression of *MIX23* in more detail. This confirmed a strong effect of cytochrome b_2-DHFR on the transcript levels of *MIX23*, which were up-regulated more than 4-fold (Fig. 2*A*). *MIX23* transcript levels were also significantly increased upon overexpression of Cox11, an endogenous protein that is synthesized with a bipartite presequence (41), albeit to a lower degree (Fig. 2*B*). Mitoprotein-induced stress was also detected in mutants of the mitochondrial TIM23 machinery (34, 42–44), and we observed increased *MIX23* levels in temperature-sensitive *tim17-5* mutants at permissive (25 °C) and semi-permissive (33 °C) temperatures (Fig. 2*C*). In contrast, *MIX23* levels were more moderately affected in a temperature-sensitive *mia40-3* mutant (Fig. 2*D*) in which the import of proteins into the IMS but not into the matrix is compromised (45).

We next tested whether *MIX23* expression is also induced upon other stress conditions. However, increased temperature did not result in *MIX23* induction, whereas the target of the heat shock response *HSP82* was induced (Fig. 2*E*). The presence of neither aggregate in the cytosol led to *MIX23* induction, because neither the overexpression of a polyQ model protein (huntingtin 97 (Htt97)-GFP) nor of α-synuclein significantly changed the transcript levels of *MIX23* (Fig. 2*F*).

Because we observed that *MIX23* is coexpressed with genes of proteasome subunits, we tested whether clogger-mediated *MIX23* induction depends on regulatory particle non-ATPase 4 (Rpn4), which serves as a master transcription factor for components of the proteasome machinery (46–48). Indeed, cytochrome b_2-DHFR expression in Δ*rpn4* cells did not induce *MIX23* (Fig. 2*G*, *cf.* Fig. 2*A*). However, overexpression of Rpn4 in yeast cells (49) induced *MIX23* expression as it does of the established Rpn4 target putative proteasome subunit 2 (*PUP2*) (Fig. 2*H*). Under the conditions here, the induction is mild (about 1.4-fold) presumably because of the fact that the levels of the Rpn4 protein are tightly regulated by a feedback mechanism (46). From this we conclude that *MIX23* and proteasome subunits are coregulated via one common transcription factor (Fig. 2*I*).

Mix23 is a Mia40 substrate of the IMS

Mix23 has been previously identified in a proteomic screen for components that are released from isolated mitochondria by a BCL2 associated X (Bax)-mediated opening of the outer membrane (39). We confirmed the localization of Mix23 in the IMS of mitochondria because it became accessible to protease after rupturing the outer membrane by hypotonic swelling (Fig. 3*A*). Mix23 homologs are found throughout fungi and animals, all containing four conserved cysteine residues (Fig. 3*B* and Fig. S1). Mix23 lacks a presequence (Fig. 3*B* and Fig. S2), and its cysteine pattern is distinct from that of the twin Cx_3C or twin Cx_9C proteins that represent well-studied substrates of the Mia40 import pathway (20).

When mitochondrial proteins were denatured with SDS and treated with the alkylating agent $mmPEG_{24}$ (methyl-PEG24-maleimide), Mix23 only shifted in size after the disulfide bonds were reduced with TCEP (tris(2-carboxyethyl)phosphine), consistent with the cysteines in endogenous Mix23 protein being oxidized (Fig. 3*C*). The formation of disulfide bonds in IMS proteins are catalyzed by the import component Mia40. Mia40 is also crucial for the import of Mix23, because mitochondria from *mia40-3* cells did not import radiolabeled Mix23 in an *in vitro* import experiment whereas mitochondria of WT cells imported Mix23 efficiently (Fig. 3*D*). The cysteine residues of Mix23 are crucial for its Mia40-dependent import because a mutant in which the six cysteine residues were replaced by serines was not imported (Fig. 3*E*). Thus, the import of Mix23 shows a similar Mia40-dependence as that of the twin Cx_3C protein Tim9 (Fig. S3*A*). Further, the import of presequence-containing proteins such as Oxa1 does not require Mia40 (Fig. S3*B*). From this we conclude that Mix23 is an IMS

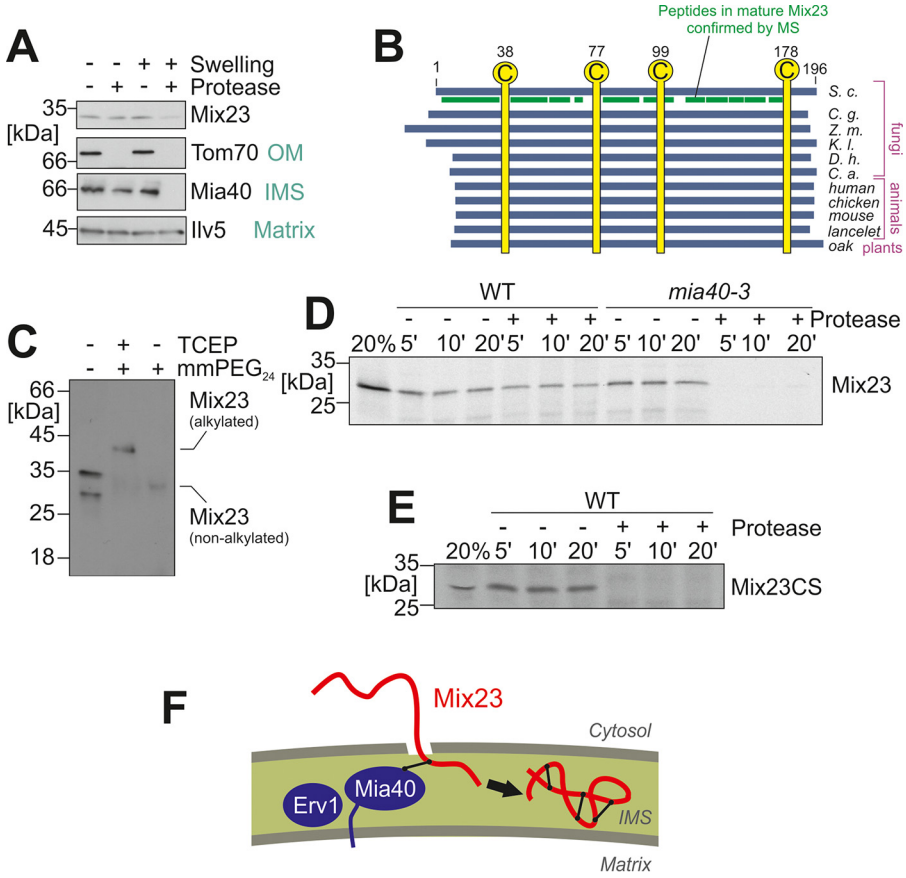

Figure 3. Mix23 IMS import is Mia40-dependent. *A*, isolated mitochondria were subfractionated by hypotonic swelling and incubation with proteinase K (protease). The matrix protein Ilv5 remained inaccessible to protease at these conditions, whereas the IMS protein Mia40 and Mix23 were digestible once the outer membrane (*OM*) was ruptured by swelling. *B*, schematic representation of Mix23 homolog sequences from different organisms (see Fig. S1 for details and nonabbreviated species names). Positions of conserved cysteine residues are indicated in *yellow*. Mix23 was isolated from yeast mitochondria and analyzed by MS. Identified peptides are shown in *green*. See Fig. S2 for details. *C*, cell extracts were treated with the reductant TCEP and the alkylating agent $mmPEG_{24}$. Mix23 was detected by Western blotting. In the presence of TCEP, but not in its absence, Mix23 was alkylated by $mmPEG_{24}$, indicating that cysteine residues are oxidized in Mix23 *in vivo*. *D*, Mix23 was synthesized in reticulocyte lysate in the presence of [^{35}S]methionine and incubated for the indicated times with mitochondria isolated from WT or *mia40-3* cells that were both grown at 33 °C. Mitochondria were isolated and treated with proteinase K where indicated. Proteins were resolved by SDS-PAGE and visualized by autoradiography. *E*, radiolabeled Mix23CS protein in which all six cysteine residues had been replaced by serine residues was incubated with WT mitochondria and further treated as described in (*D*). *F*, schematic representation of the Mia40-mediated import of Mix23 into the IMS, also showing the mixed disulfide form as a reaction intermediate.

protein with a conserved pattern of cysteine residues that is imported into mitochondria via the Mia40 disulfide relay (Fig. 3*F*).

High Mix23 levels lead to a severe growth defect

As reported above, mitoprotein-induced stress leads to a considerable up-regulation of Mix23. We therefore tested the effects of increased levels of Mix23 by expression of the protein from a regulatable galactose metabolism 1 (*GAL1*) promoter (Mix23↑). In the presence of galactose, where Mix23 levels are strongly increased, we observed a considerable reduction in growth of Mix23↑ cells irrespective of temperature (Fig. 4*A* and Fig. S3*D*). Obviously, increased amounts of Mix23 are not well tolerated by yeast cells, potentially because the unphysiologically high levels of Mix23 clog the import machinery. A hallmark of the mitoprotein-induced stress response triggered by cloggers is the induction of the Rpn4 response (33). Indeed, we observed that Mix23↑ strongly induced the expression of a YFP reporter from a reporter that contains the proteasome-associated control element (PACE) to which Rpn4 binds (Fig. 4*B*). Because yeast cells can grow by fermentation on galactose plates, the slow growth is not due to defects in respiration but rather in a function of more general relevance.

We therefore tested whether increased levels of Mix23 interfere with the import of proteins into isolated mitochondria. Interestingly, we found that the import of the matrix protein Atp1 and the inner membrane protein Oxa1 into Mix23↑ mitochondria was strongly diminished (Fig. 4, *C–F*). Similarly, the import of the IMS protein Cmc1 into Mix23↑ mitochondria was reduced (Fig. 4, *G* and *H*).

It was shown before that IMS proteins that fail to be imported into mitochondria are degraded by the proteasome (50–52). The Mia40 substrate Cox12 was identified as a protein that is particularly unstable in the cytosol but stable in the IMS so that its stability can be used to monitor its intracellular distribution (53, 54). We therefore tagged Cox12 by chromosomal integration of an HA epitope in WT or Mix23↑ cells. When synthesis of new proteins was inhibited by addition of cycloheximide, Cox12 remained stable in the WT cells but was rapidly degraded in the Mix23↑ mutant (Fig. 4*I*). The matrix protein

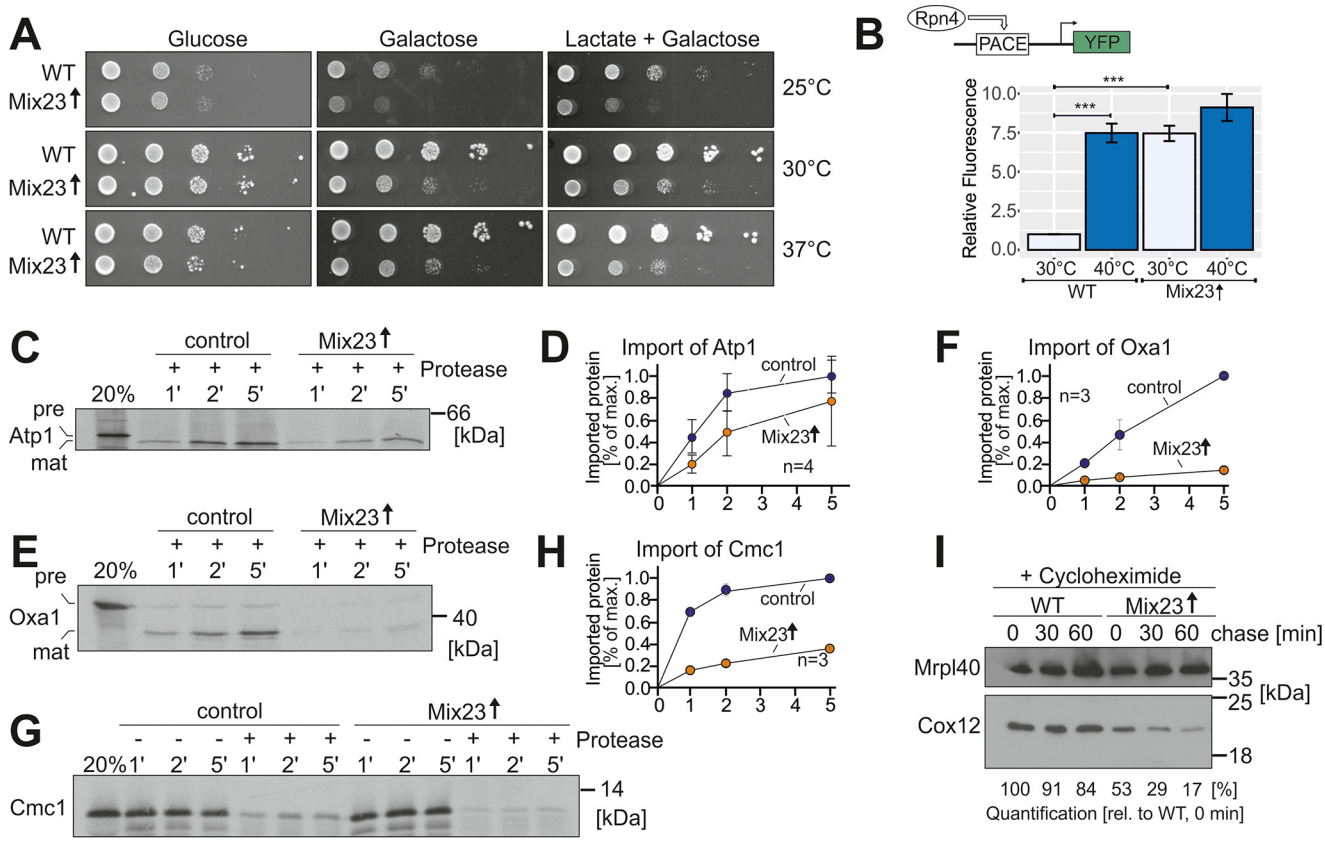

Figure 4. Increased levels of Mix23 inhibit the import of proteins into mitochondria. *A*, the cells were transformed with an empty (WT) or a *GAL1-MIX23* plasmid (Mix23↑) and grown to mid-log phase before 10-fold serial dilutions were dropped on the indicated plates. Note that the overexpression of Mix23 retarded cell growth independent of the temperature. *B*, the cells expressing YFP under control of an Rpn4-driven PACE element and a minimal promoter were transformed with an empty or the Mix23↑ plasmid and grown on synthetic lactate at 30 or 40 °C. 3 h after induction by addition of 0.5% galactose, the fluorescence of YFP was measured. Means and S.D. of nine (three technical and three biological) replicates are shown. Mix23 overexpression leads to a strong Rpn4-driven gene expression already at 30 °C. *C–G*, mitochondria were isolated from WT and Mix23↑ cells. Radiolabeled precursor forms of the matrix protein Atp1, the inner membrane protein Oxa1, and the IMS protein Cmc1 were incubated with these mitochondria for the times indicated before non-imported material was removed by protease treatment. Overexpression of Mix23 interfered with the efficient import of all three proteins. *I*, cells expressing an HA-tagged version of Cox12 were transformed with an empty plasmid (WT) or the *GAL1-MIX23* plasmid (Mix23↑). The cells were grown on lactate medium containing 0.5% galactose. Then cycloheximide was added to block protein synthesis. Aliquots were taken at the indicated times. The cells were lysed and Cox12 levels were analyzed by Western blotting. Note that upon overexpression of Mix23, Cox12 is highly unstable and rapidly degraded.

mitochondrial ribosomal protein L40 (Mrpl40) served as a control in this experiment and was not degraded by Mix23 overexpression. Thus, in summary, we found that the synthesis of high amounts of Mix23 interferes with the translocation of proteins into mitochondria.

Mix23 is required for efficient preprotein import into tim17-5 mitochondria

Next, we tested the relevance of Mix23 for mitochondrial functionality. Mutants lacking Mix23 did not show growth defects on fermentative and nonfermentative carbon sources, and the import or oxidation of matrix and IMS proteins was not perturbed in the Δ*mix23* single mutant (Fig. 5 and Fig. S4, *A–E*).

However, when *MIX23* was deleted in the background of a temperature-sensitive *tim17-5* mutant, a synthetic growth defect was observed even on fermentative glucose medium at permissive temperatures (25 and 30 °C). Under these conditions, the *tim17-5* mutant grew indistinguishable from WT cells. The *tim17-5* Δ*mix23* mutant still grew at these conditions, albeit with reduced colony size (Fig. 5*B*). No synthetic defect was observed when Mix23 was deleted in a temperature-sensitive *mia40-3* mutant (Fig. S3*C*), suggesting that Mix23 is particularly relevant for matrix targeting but not for the biogenesis of IMS proteins using the mitochondrial disulfide relay.

This synthetic genetic interaction of *MIX23* and *TIM17* was confirmed by *in vitro* import experiments. The import of Oxa1 and Atp1 into *tim17-5* Δ*mix23* double mutant mitochondria was considerably reduced, particularly at elevated temperatures (Fig. 5, *C–F* and Fig. S5, *A–D*), whereas the single mutants were either not affected or less affected. The import of the Mia40 substrate Cx_9C motif containing protein 1 (Cmc1) was not diminished in the *tim17-5* Δ*mix23* mitochondria, confirming a specific relevance of Mix23 for matrix-destined proteins (Fig. 5, *G* and *H* and Fig. S5, *E* and *F*). It should be noted that *tim17-5* Δ*mix23* mitochondria were isolated from cells that were grown at permissive temperature (25 °C) at which the *tim17-5* mutant shows no obvious difference from WT cells (44). Apparently, efficient Oxa1 import into the matrix of *tim17-5* mitochondria requires Mix23.

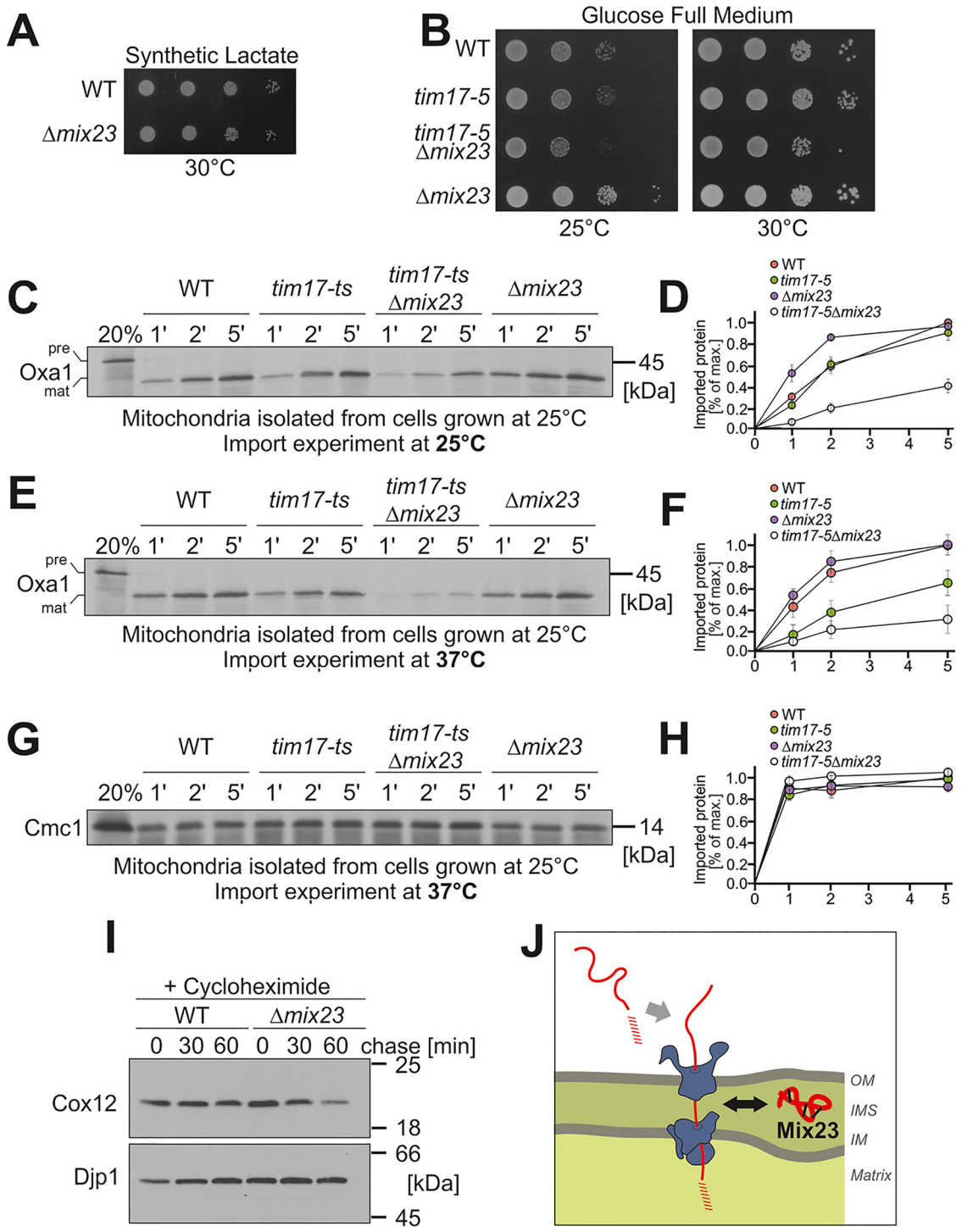

Figure 5. Mix23 facilitates efficient protein import into mitochondria. *A*, WT and Δ*mix23* cells were grown on synthetic lactate medium to log phase. Then 10-fold serial dilutions were dropped onto synthetic lactate (2%) medium. *B*, *MIX23* was deleted in the background of the temperature-sensitive *tim17-5* mutant. The resulting double mutant (and *tim17-5* cells for control) was analyzed by a drop dilution assay on full glucose medium and grown at the temperatures indicated. *C–H*, mitochondria were isolated from the strains indicated grown at permissive temperature (25 °C). Radiolabeled Oxa1 and Cmc1 proteins were incubated with these mitochondria at the temperatures indicated. *I*, the cells were grown on glycerol-containing medium. Protein synthesis was inhibited by addition of cycloheximide. Samples were taken 0, 30, and 60 min after cycloheximide addition. The cells were lysed and the levels of Cox12 and the loading control Djp1 were analyzed by Western blotting. *J*, model of a role of Mix23 as a factor that directly or indirectly influences the efficiency of mitochondrial protein import.

This suggests that Mix23 has a stabilizing or stimulating activity on mitochondrial protein import. This is also supported by the observation that Cox12 has a much lower stability in Δ*mix23* cells, in line with a less efficient protein import in this *in vivo* model (Fig. 5*I*). From these results we conclude that Mix23 is not essential for mitochondrial protein import *per se* but stimulates or stabilizes protein translocation (Fig. 5*J*).

Discussion

The mitochondrial IMS contains a number of small cysteine-containing proteins that are imported by Mia40. In yeast, where IMS proteins are best characterized, Mia40 clients comprise five twin Cx_3C proteins, about 15 Cx_9C proteins, and a small number of proteins with cysteine residues in other arrangements (25, 26, 39, 55). Here we show that Mix23 is a further Mia40 substrate of the IMS whose cysteine residues do not match the Cx_nC pattern. The Mia40-driven import of Mix23 into the IMS depends on its cysteine residues because a cysteine-less mutant was not import-competent.

In yeast, Mix23 has six cysteine residues, four of which are conserved. Mix23 homologs are found ubiquitously in fungi and animals (many hundred homologous sequences in NCBI). In humans, the Mix23-like protein was named coiled-coil domain containing 58, CCDC58. This protein is localized to mitochondria and found to interact with a number of IMS proteins, including ATPase family gene 3 like 2 (AFG3L2), apoptosis inducing factor mitochondria associated 1 (AIFM1), synthesis of SCO1, and cytochrome c in recent high-throughput interaction studies (56–58). Its function is elusive, but increased CCDC58 levels have been identified as an unfavorable prognostic factor in endometrial hyperplasia (59) and in liver and urothelial cancer (60) (RRID:SCR_006710). Consequently, a role for CCDC58 in tumor progression was suggested. Moreover, CCDC58 was identified as one of a few cellular proteins whose absence provides resistance against the intracellular bacterium *Ehrlichia chaffeensis*, the cause of monocytic ehrlichiosis (61).

Despite this pathophysiological relevance and although CCDC58 is expressed in a wide variety of tissues in mice and humans, including skeletal muscle, heart, and brain, (62, 63), mice lacking CCDC58 were healthy and free of obvious symptoms (64). Thus, increased levels of CCDC58 were associated with pathological conditions in cancer or pathogen-infected cells, but its absence is obviously well tolerated under nonstress conditions. This is reminiscent of what we observed in this study. Yeast cells lacking Mix23 did only show mild defects, whereas overexpression of Mix23 strongly affected cellular functionality. However, it should be noted that the overexpression used in this study is certainly higher than that under physiological conditions even in stressed cells.

The expression of Mix23 was strongly and specifically increased by mitoprotein-induced stress, a condition that both up-regulates (33) and activates (34) the cytosolic proteasome system. Moreover, we found that Mix23 expression depends on Rpn4, the master transcription factor of the proteasome system in yeast (46, 49). Thus, Mix23 serves as a stress-induced factor that is coregulated with the proteasome. The coregulation of *MIX23* and proteasome components is also apparent from the Serial Pattern of Expression Levels Locator database, which calculates coexpression scores on the basis of hundreds of gene expression microarray data (65). Here, *MIX23* showed a coexpression with genes with a Gene Ontology (GO) annotation "mitochondrial protein complex," "mitochondrial large ribosomal subunit," "mitochondrial small ribosomal subunit," and "proteasome complex," in line with a role in mitochondrial biogenesis and proteostasis (Fig. S6). However, the fact that Mix23 and the proteasome are under regulation of the same transcription factor Rpn4 alone is not convincing evidence for a function of Mix23 in protein quality control, but just shows that the regulation of their cellular abundance adheres to similar regulatory patterns.

The molecular function of Mix23 in the IMS and the reasons that this factor is up-regulated during mitoprotein-induced stress remain unclear. An Rpn4-dependent regulation was also described before for Mia40 (33, 66, 67). Still, we found no indication that Mix23 is of relevance for the functionality of the mitochondrial disulfide relay in the IMS, and the deletion of *MIX23* did not lead to synthetic defects in *mia40-3* mutants. However, the observed synthetic defect with the *tim17-5* mutation suggests that Mix23 facilitates the import of presequence-containing proteins (Fig. 5*F*). Such a role might be direct, for example by interaction with IMS-exposed regions of the TOM or the TIM23 subunits, which are well-known to be part of a highly complex network of regulatory interactions (9–13). But this role also could be more indirect, for example by an effect of Mix23 on the local distribution of the translocases and their interaction with proteins and lipids of the outer and inner membranes. Several examples for such modulating factors that influence the import machinery were reported in recent years, such as Tim21 or Mgr2 (10, 11, 44, 68, 69).

It will be interesting to unravel the molecular mechanisms in detail by which Mix23 regulates mitochondrial protein translocation and, in particular, its specific function in the context of the cytosolic stress conditions that coregulate it together with the proteasome and other Rpn4 targets.

Experimental procedures

Yeast strains and plasmids

All yeast strains used in this study are based on the WT strains BY4742 (MATα *his3 leu2 lys2 ura3*), YPH499 (MATa *ura3 lys2 ade2 trp1 his3 leu2*), or YPH499 Δ*arg4* (MATα *ura3 lys2 ade2 trp1 his3 leu2 arg4*).

The *mia40*-3 and *tim17*-5 mutants were described previously (44, 45). For the detection of Cox12 and Mix23 in Western blotting, a *HIS3*MX6 cassette was genomically integrated downstream of the *COX12* and *MIX23* loci, respectively (70). The mutants *tim17-5* Δ*mix23* and *mia40-3* Δ*mix23* were generated by genomically integrating the NatNT2 cassette into the *MIX23* ORF. Positive colonies were verified by PCR.

For generation of the Mix23CS mutant, a variation of the *MIX23* DNA sequence was synthesized in which all cysteine-specific codons were replaced by those for serine. This sequence was cloned into pGEM4 using the restriction sites EcoRI and BamHI. The plasmid was verified by sequencing.

To generate a Mix23 overexpression plasmid, the coding region of *MIX23* was amplified from genomic DNA and ligated into a pYX223 empty vector plasmid between the *GAL1* promoter and an HA tag by using the restriction sites EcoRI and SalI. For the Rpn4 activity reporter, the *MIX23* sequence was cloned into a p426 *GAL1* vector, and a pNH603 PACE-YFP reporter plasmid was used as described before (33).

To produce radiolabeled lysate of Mix23, the coding region of *MIX23* was amplified from genomic DNA and cloned into a

pGEM4 plasmid using the restriction sites EcoRI and XmaI. All plasmids were verified by sequencing.

All yeast strains used in this study are listed in Table S1. Strains were grown in yeast complete medium (1% yeast extract and 2% peptone) containing 2% of the carbon sources galactose, glucose, or glycerol as indicated. Temperature-sensitive strains (*mia40-3* and *tim17-5*) were grown at 25 °C before switching them to 33 °C. Strains containing plasmids were grown at 30 °C in minimal synthetic medium containing 0.67% yeast nitrogen base and 2% lactate as carbon source. To induce the expression from the *GAL1* promoter, cultures were supplemented with 0.5% galactose.

Drop dilution assay

To test growth on plates, drop dilution assays were conducted. Yeast cells were grown in YPGal media or lactate selective media to mid-log phase. After harvesting 1 OD600 of cells and washing with sterile water, a 1:10 serial dilution was prepared in sterile water. Equal amounts of the dilutions were dropped on agar plates to determine growth differences. Pictures of the plates were taken after 2 to 3 days of incubation.

Growth curve assay

To test growth in liquid media, growth curves were performed. Yeast cells were grown in lactate selective media to mid-log phase. After harvesting 0.1 OD600 of cells and washing with sterile water, the cell pellets were resuspended in the experimental media and transferred into a clear 96-well plate. Automated *A* measurements were performed at 600 nm in the ELx808™ Absorbance Microplate Reader (BioTek®). *A*s were measured for 72 h every 10 min at 30 °C in technical triplicates.

Analysis of mRNA levels by quantitative real-time PCR

To determine relative mRNA expression levels, quantitative real-time PCR was conducted. Yeast strains were treated as indicated and grown until mid-log phase before RNA isolation. The equivalents of two optical densities (600 nm) were used for each RNA sample. RNA isolation was performed using the RNeasy Mini Kit (Qiagen) with a column DNase digestion (Qiagen). 500 ng of each RNA sample were used to synthesize complementary DNA with a qScript™ cDNA Synthesis Kit (Quantabio). To measure relative mRNA levels, the iTaq Universal SYBR Green Supermix (Bio-Rad) was used with 2 µl of a 1 in 10 dilution of cDNA. Measurements were performed in technical triplicates with the CFX96 Touch Real-Time PCR Detection System (Bio-Rad). Relative mRNA expression was calculated by the $2^{-\Delta\Delta CT}$ method (71). For normalization, the housekeeping genes *TFC1* or *TFA2* were used because of their stability in published gene expression data (72). See Table S3 for primer sequences.

Statistical significance was assessed using a paired one-tailed Student's *t* test.

Cox12 degradation assay

To investigate the role of Mix23 in the degradation of mitochondrial proteins of the IMS, a Cox12 degradation assay was carried out essentially as previously described (54). Cells expressing Cox12-HA were grown in yeast complete medium containing 2% glycerol (or synthetic lactate medium with 0.5% galactose in case of the Mix23 overexpression strain) before 0.1 mg/ml cycloheximide was added to stop protein translation. Whole cell lysates were taken over time and visualized by Western blotting.

Isolation of mitochondria

To isolate crude mitochondria, yeast strains were cultivated either in full or selective media under respiratory conditions. The cells were grown to mid-log phase and harvested by centrifugation (5 min, 3000 × *g*). After washing the pellets with water and centrifugation (5 min, 3000 × *g*), the weight of the cell pellet was determined. The pellets were resuspended in 2 ml/g wet weight MP1 (100 mM Tris and 10 mM DTT), incubated for 10 min at 30 °C, and centrifuged again (5 min, 3000 × *g*). The pellets were washed with 1.2 M sorbitol and centrifuged (5 min, 3000 × *g*) before resuspending in 6.7 ml/g wet weight MP2 (20 mM KPi buffer, pH 7.4, 1.2 M sorbitol, and 3 mg/g wet weight zymolyase from Seikagaku Biobusiness) and incubated at 30 °C for 60 min. The following steps were conducted on ice. After centrifugation (5 min, 2800 × *g*), the pellets were resuspended in 13.4 ml/g wet weight homogenization buffer (10 mM Tris, pH 7.4, 1 mM EDTA, 0.2% BSA, 1 mM PMSF, and 0.6 M sorbitol), and a cooled glass potter was used to homogenize the sample with 10 strokes. After homogenization, the extract was centrifuged three times (5 min, 2800 × *g*) while always keeping the mitochondria-containing supernatant. To pellet mitochondria, the samples were centrifuged for 12 min at 17,500 × *g*. The pellets were resuspended in SH buffer (0.6 M sorbitol and 20 mM HEPES, pH 7.4). The concentration of the purified mitochondria was adjusted to 10 µg/ml protein. Aliquots were snap-frozen in liquid nitrogen and stored at −80 °C.

Import of radiolabeled precursor proteins into mitochondria

To prepare radiolabeled ([^{35}S]methionine) proteins for import experiments, the TNT® Quick Coupled Transcription/Translation Kit from Promega was used. To determine the ability of proteins to be imported into mitochondria, *in vitro* import assays were conducted. Mitochondria were resuspended in a mixture of import buffer (500 mM sorbitol, 50 mM Hepes, pH 7.4, 80 mM KCl, 10 mM Mg(OAc)2, and 2 mM KPi) with 2 mM ATP and 2 mM NADH to energize them for 10 min at 25 °C. To start the import, the radiolabeled lysate was added to the mitochondria. Import was stopped at different time points by transferring the mitochondria into cold SH buffer (0.6 M sorbitol and 20 mM HEPES, pH 7.4). The remaining precursors outside of the mitochondria were removed by protease treatment for 30 min. 2 mM PMSF was added to stop protein degradation. After centrifugation (10 min, 25,000 × *g*, 4 °C), the supernatant was removed. The pellets were resuspended in SH buffer containing 500 mM KCl and 2 mM PMSF and centrifuged again (10 min, 25,000 × *g*, 4 °C). The pellets were then lysed in 1× Laemmli buffer containing 50 mM DTT and heated to 96 °C for 3 min. The samples were run on a 16%

SDS-gel, blotted onto a nitrocellulose membrane, and visualized with autoradiography.

Cysteine redox state detection by mmPEG$_{24}$ shifts

To determine the oxidative state of proteins, mmPEG$_{24}$ shifts were conducted. mmPEG$_{24}$ binds to reduced thiols, inducing a size shift on SDS gels. For each free thiol, the addition of mmPEG$_{24}$ increases the size of the protein by 1.2 kDa. Mitochondria were incubated in 80 mM Tris, pH 7, 10% glycerol, 2% SDS, and 0.05% bromocresol blue. Then, mmPEG$_{24}$ was added to alkylate free thiols. To gain a maximum shift (all thiols reduced), the reducing agent tris(2-carboxyethyl)phosphine was added to a control sample before the mmPEG$_{24}$ treatment to reduce all disulfide bonds. The samples were analyzed by Western blotting.

Mitochondrial subfractionation

To determine the localization of Mix23 inside mitochondria, a swelling assay was performed. Here, reduced osmolarity of the HEPES buffer causes swelling and subsequent rupture of the outer membrane of mitochondria. Protease treatment subsequently digests proteins of the outer membrane and the IMS. Therefore, mitochondria were incubated on ice in either SH buffer (no swelling) or 20 mM HEPES buffer (swelling and rupture) with and without the presence of 100 μg/ml proteinase K. After 30 min, SH buffer with 20 mM PMSF was added. Mitochondria were then pelleted by centrifugation (10 min, 14,000 rpm, 4 °C). The pellets were resuspended in Laemmli buffer containing 50 mM DTT, heated at 96 °C for 3 min, and visualized by Western blotting.

YFP reporter assay

The cells were grown to mid-log phase (OD600 value of 0.5–0.8) in selective lactate medium. 3 h after addition of galactose, equal amounts of cells (4 OD600 × ml) were collected by centrifugation (20,000 × *g*, 5 min, room temperature), resuspended in 400 μl synthetic defined medium (100 μl per OD600 and OD600 × ml). 100 μl of this cell suspension were transferred to flat-bottomed black 96-well imaging plates (BD Falcon) in technical replicates. The cells were sedimented by gentle spinning (30 × *g*, 5 min, room temperature), and fluorescence (excitation 497 nm, emission 540 nm) was measured using a ClarioStar Fluorescence plate reader (BMG Labtech). A corresponding WT strain not expressing YFP was used for background subtraction of autofluorescence. Statistical significance was assessed using a paired one-tailed Student's *t* test.

Identification of coexpressed genes and GO enrichment analysis

To identify genes coexpressed with *MIX23* across all transcriptomics datasets deposited in the yeast *Saccharomyces* genome database, the Serial Pattern of Expression Levels Locator database (65) was queried for *MIX23* with the online interface provided by the *Saccharomyces* genome database (https://spell.yeastgenome.org). Genes with an adjusted correlation score of at least 1.4 were considered as coexpressed with *MIX23* and subjected to a GO enrichment analysis with GOrilla (RRID: SCR_006848) (73). The 170 coexpressed genes and *MIX23* were set as an unranked target list, and the complete *Saccharomyces cerevisiae* genome was set as the background list. *p* values for enrichment were calculated according to a hypergeometric distribution and corrected for multiple testing using the Benjamini-Hochberg procedure.

Whole cell lysates

To determine the protein levels of whole cells, whole cell lysates were prepared. To do so, yeast at an *A* of 1.5 (600 nm) were harvested and washed with water. The pellets were resuspended in Laemmli buffer containing 50 mM DTT. After adding glass beads, the cells were lysed using a cell beater at 4 °C. Then, the cells were heated at 96 °C for 3 min. Lysates were stored at −20 °C until visualization by Western blotting.

Antibodies

Antibodies were produced in rabbits using recombinant purified proteins (see Table S4). Secondary antibodies were ordered from Bio-Rad (Goat Anti-Rabbit IgG (H + L)-HRP Conjugate). The horseradish peroxidase–coupled HA antibody for Western blotting was obtained from Roche (Anti-HA-Peroxidase, High Affinity (3F10), catalog no. 12013819001). The Anti-HA agarose antibody for immunoprecipitation was obtained from Sigma-Aldrich (monoclonal Anti-HA agarose antibody produced in mouse, A2095). Antibodies were diluted in 5% nonfat dry milk-TBS (Roth, T145.2).

Data availability

All relevant data for this study are contained within this article and in the supporting information. Materials and strains are available from the authors.

Acknowledgments—We thank Sabine Knaus, Vera Nehr, and Hannah Otto for technical assistance, Ralf Braun (Krems, Austria) for reagents, and Zuzana Storchova and Bruce Morgan for critical reading of the manuscript.

Author contributions—E. Z., J. L., F. B., R. T. A., and J. M. H. conceptualization; E. Z., J. L., L. K., F. B., M. R., and J. M. H. data curation; E. Z., J. L., L. K., and F. B. formal analysis; E. Z., J. L., L. K., F. B., and M. R. validation; E. Z., J. L., F. B., M. R., and J. M. H. investigation; E. Z., J. L., F. B., and R. T. A. methodology; E. Z., J. L., L. K., F. B., R. T. A., and J. M. H. writing-review and editing; F. B. resources; F. B. software; J. M. H. supervision; J. M. H. funding acquisition; J. M. H. writing-original draft; J. M. H. project administration.

Funding and additional information—This project was funded by the German Research Foundation Grants DIP MitoBalance, SPP1710, IRTG1830, HE2803/8-2 (to J. M. H.), and FOR2800 (to M. R.), the Landesschwerpunkt BioComp (to J. M. H.), and the Joachim Herz Foundation (to F. B.).

Conflict of interest—The authors declare that they have no conflicts of interest with the contents of this article.

Abbreviations—The abbreviations used are: IMS, intermembrane space; TIM, translocase of the inner membrane; MTSs, matrix targeting signals; TOM, translocase of the outer mitochondrial membrane; DHFR, dihydrofolate reductase; mmPEG, methyl-PEG-maleimide; TCEP, tris(2-carboxyethyl)phosphine; PACE, proteasome-associated control element.

References

1. Avendaño-Monsalve, M. C., Ponce-Rojas, J. C., and Funes, S. (2020) From cytosol to mitochondria: the beginning of a protein journey. *Biol. Chem.* **401,** 645–661 CrossRef Medline
2. Bykov, Y. S., Rapaport, D., Herrmann, J. M., and Schuldiner, M. (2020) Cytosolic events in the biogenesis of mitochondrial proteins. *Trends Biochem. Sci.* **45,** 650–667 CrossRef Medline
3. Bausewein, T., Mills, D. J., Langer, J. D., Nitschke, B., Nussberger, S., and Kühlbrandt, W. (2017) Cryo-EM structure of the TOM core complex from *Neurospora crassa*. *Cell* **170,** 693–700 CrossRef Medline
4. Araiso, Y., Tsutsumi, A., Qiu, J., Imai, K., Shiota, T., Song, J., Lindau, C., Wenz, L. S., Sakaue, H., Yunoki, K., Kawano, S., Suzuki, J., Wischnewski, M., Schutze, C., Ariyama, H., *et al.* (2019) Structure of the mitochondrial import gate reveals distinct preprotein paths. *Nature* **575,** 395–401 CrossRef Medline
5. Tucker, K., and Park, E. (2019) Cryo-EM structure of the mitochondrial protein-import channel TOM complex at near-atomic resolution. *Nat. Struct. Mol. Biol.* **26,** 1158–1166 CrossRef Medline
6. Shiota, T., Imai, K., Qiu, J., Hewitt, V. L., Tan, K., Shen, H. H., Sakiyama, N., Fukasawa, Y., Hayat, S., Kamiya, M., Elofsson, A., Tomii, K., Horton, P., Wiedemann, N., Pfanner, N., *et al.* (2015) Molecular architecture of the active mitochondrial protein gate. *Science* **349,** 1544–1548 CrossRef Medline
7. Moro, F., Sirrenberg, C., Schneider, H.-C., Neupert, W., and Brunner, M. (1999) The TIM17·23 preprotein translocase of mitochondria: composition and function in protein transport of mitochondria. *EMBO J.* **18,** 3667–3675 CrossRef Medline
8. Voisine, C., Craig, E. A., Zufall, N., von Ahsen, O., Pfanner, N., and Voos, W. (1999) The protein import motor of mitochondria: unfolding and trapping of preproteins are distinct and separable functions of matrix Hsp70. *Cell* **97,** 565–574 CrossRef Medline
9. Lytovchenko, O., Melin, J., Schulz, C., Kilisch, M., Hutu, D. P., and Rehling, P. (2013) Signal recognition initiates reorganization of the presequence translocase during protein import. *EMBO J.* **32,** 886–898 CrossRef Medline
10. Chacinska, A., van der Laan, M., Mehnert, C. S., Guiard, B., Mick, D. U., Hutu, D. P., Truscott, K. N., Wiedemann, N., Meisinger, C., Pfanner, N., and Rehling, P. (2010) Distinct forms of mitochondrial TOM-TIM supercomplexes define signal-dependent states of preprotein sorting. *Mol. Cell Biol.* **30,** 307–318 CrossRef Medline
11. Popov-Celeketić, D., Mapa, K., Neupert, W., and Mokranjac, D. (2008) Active remodelling of the TIM23 complex during translocation of preproteins into mitochondria. *EMBO J.* **27,** 1469–1480 CrossRef Medline
12. Caumont-Sarcos, A., Moulin, C., Poinot, L., Guiard, B., van der Laan, M., and Ieva, R. (2020) Transmembrane coordination of preprotein recognition and motor coupling by the mitochondrial presequence receptor Tim50. *Cell Rep.* **30,** 3092–3104 CrossRef Medline
13. Callegari, S., Cruz-Zaragoza, L. D., and Rehling, P. (2020) From TOM to the TIM23 complex - handing over of a precursor. *Biol. Chem.* **401,** 709–721 CrossRef Medline
14. Tienson, H. L., Dabir, D. V., Neal, S. E., Loo, R., Hasson, S. A., Boontheung, P., Kim, S. K., Loo, J. A., and Koehler, C. M. (2009) Reconstitution of the mia40-erv1 oxidative folding pathway for the small tim proteins. *Mol. Biol. Cell* **20,** 3481–3490 CrossRef Medline
15. Mesecke, N., Terziyska, N., Kozany, C., Baumann, F., Neupert, W., Hell, K., and Herrmann, J. M. (2005) A disulfide relay system in the intermembrane space of mitochondria that mediates protein import. *Cell* **121,** 1059–1069 CrossRef Medline
16. Naoé, M., Ohwa, Y., Ishikawa, D., Ohshima, C., Nishikawa, S., Yamamoto, H., and Endo, T. (2004) Identification of Tim40 that mediates protein sorting to the mitochondrial intermembrane space. *J. Biol. Chem.* **279,** 47815–47821 CrossRef Medline
17. Edwards, R., Gerlich, S., and Tokatlidis, K. (2020) The biogenesis of mitochondrial intermembrane space proteins. *Biol. Chem.* **401,** 737–747 CrossRef Medline
18. Finger, Y., and Riemer, J. (2020) Protein import by the mitochondrial disulfide relay in higher eukaryotes. *Biol. Chem.* **401,** 749–763 CrossRef Medline
19. Milenkovic, D., Ramming, T., Müller, J. M., Wenz, L. S., Gebert, N., Schulze-Specking, A., Stojanovski, D., Rospert, S., and Chacinska, A. (2009) Identification of the signal directing Tim9 and Tim10 into the intermembrane space of mitochondria. *Mol. Biol. Cell* **20,** 2530–2539 CrossRef Medline
20. Sideris, D. P., Petrakis, N., Katrakili, N., Mikropoulou, D., Gallo, A., Ciofi-Baffoni, S., Banci, L., Bertini, I., and Tokatlidis, K. (2009) A novel intermembrane space-targeting signal docks cysteines onto Mia40 during mitochondrial oxidative folding. *J. Cell Biol.* **187,** 1007–1022 CrossRef Medline
21. Peleh, V., Cordat, E., and Herrmann, J. M. (2016) Mia40 is a trans-site receptor that drives protein import into the mitochondrial intermembrane space by hydrophobic substrate binding. *eLife* **5,** e16177 CrossRef
22. Peleh, V., Zannini, F., Backes, S., Rouhier, N., and Herrmann, J. M. (2017) Erv1 of Arabidopsis thaliana can directly oxidize mitochondrial intermembrane space proteins in the absence of redox-active Mia40. *BMC Biol.* **15,** 106 CrossRef Medline
23. Banci, L., Bertini, I., Cefaro, C., Ciofi-Baffoni, S., Gallo, A., Martinelli, M., Sideris, D. P., Katrakili, N., and Tokatlidis, K. (2009) Mia40 is an oxidoreductase that catalyzes oxidative protein folding in mitochondria. *Nat. Struct. Mol. Biol.* **16,** 198–206 CrossRef Medline
24. Allen, S., Lu, H., Thornton, D., and Tokatlidis, K. (2003) Juxtaposition of the two distal CX3C motifs via intrachain disulfide bonding is essential for the folding of Tim10. *J. Biol. Chem.* **278,** 38505–38513 CrossRef Medline
25. Gabriel, K., Milenkovic, D., Chacinska, A., Müller, J., Guiard, B., Pfanner, N., and Meisinger, C. (2007) Novel mitochondrial intermembrane space proteins as substrates of the MIA import pathway. *J. Mol. Biol.* **365,** 612–620 CrossRef Medline
26. Longen, S., Bien, M., Bihlmaier, K., Kloeppel, C., Kauff, F., Hammermeister, M., Westermann, B., Herrmann, J. M., and Riemer, J. (2009) Systematic analysis of the twin Cx_9C protein family. *J. Mol. Biol.* **393,** 356–368 CrossRef Medline
27. Weinhäupl, K., Lindau, C., Hessel, A., Wang, Y., Schütze, C., Jores, T., Melchionda, L., Schönfisch, B., Kalbacher, H., Bersch, B., Rapaport, D., Brennich, M., Lindorff-Larsen, K., Wiedemann, N., and Schanda, P. (2018) structural basis of membrane protein chaperoning through the mitochondrial intermembrane Space. *Cell* **175,** 1365–1379 CrossRef Medline
28. Ramesh, A., Peleh, V., Martinez-Caballero, S., Wollweber, F., Sommer, F., van der Laan, M., Schroda, M., Alexander, R. T., Campo, M. L., and Herrmann, J. M. (2016) A disulfide bond in the TIM23 complex is crucial for voltage gating and mitochondrial protein import. *J. Cell Biol.* **214,** 417–431 CrossRef Medline
29. Wrobel, L., Trojanowska, A., Sztolsztener, M. E., and Chacinska, A. (2013) Mitochondrial protein import: Mia40 facilitates Tim22 translocation into the inner membrane of mitochondria. *Mol. Biol. Cell* **24,** 543–554 CrossRef Medline
30. Okamoto, H., Miyagawa, A., Shiota, T., Tamura, Y., and Endo, T. (2014) Intramolecular disulfide bond of Tim22 protein maintains integrity of the TIM22 complex in the mitochondrial inner membrane. *J. Biol. Chem.* **289,** 4827–4838 CrossRef Medline
31. Weckbecker, D., Longen, S., Riemer, J., and Herrmann, J. M. (2012) Atp23 biogenesis reveals a chaperone-like folding activity of Mia40 in the IMS of mitochondria. *EMBO J.* **31,** 4348–4358 CrossRef Medline

32. Weidberg, H., and Amon, A. (2018) MitoCPR-A surveillance pathway that protects mitochondria in response to protein import stress. *Science* **360,** eaan4146 CrossRef Medline
33. Boos, F., Krämer, L., Groh, C., Jung, F., Haberkant, P., Stein, F., Wollweber, F., Gackstatter, A., Zöller, E., van der Laan, M., Savitski, M. M., Benes, V., and Herrmann, J. M. (2019) Mitochondrial protein-induced stress triggers a global adaptive transcriptional programme. *Nat. Cell Biol.* **21,** 442–451 CrossRef Medline
34. Wrobel, L., Topf, U., Bragoszewski, P., Wiese, S., Sztolsztener, M. E., Oeljeklaus, S., Varabyova, A., Lirski, M., Chroscicki, P., Mroczek, S., Januszewicz, E., Dziembowski, A., Koblowska, M., Warscheid, B., and Chacinska, A. (2015) Mistargeted mitochondrial proteins activate a proteostatic response in the cytosol. *Nature* **524,** 485–488 CrossRef Medline
35. Mårtensson, C. U., Priesnitz, C., Song, J., Ellenrieder, L., Doan, K. N., Boos, F., Floerchinger, A., Zufall, N., Oeljeklaus, S., Warscheid, B., and Becker, T. (2019) Mitochondrial protein translocation-associated degradation. *Nature* **569,** 679–683 CrossRef Medline
36. Shakya, V. P. S., Barbeau, W. A., Xiao, T., Knutson, C. S., and Hughes, A. L. (2020) The nucleus is a quality control center for non-imported mitochondrial proteins. *bioRxiv* CrossRef
37. Xiao, T., Shakya, V. P. S., and Hughes, A. L. (2020) The GET pathway safeguards against non-imported mitochondrial protein stress. *bioRxiv* CrossRef
38. Boos, F., Labbadia, J., and Herrmann, J. M. (2020) How the mitoprotein-induced stress response safeguards the cytosol: a unified view. *Trends Cell Biol.* **30,** 241–254 CrossRef Medline
39. Vögtle, F. N., Burkhart, J. M., Rao, S., Gerbeth, C., Hinrichs, J., Martinou, J. C., Chacinska, A., Sickmann, A., Zahedi, R. P., and Meisinger, C. (2012) Intermembrane space proteome of yeast mitochondria. *Mol. Cell. Proteomics* **11,** 1840–1852 CrossRef Medline
40. Pfeffer, S., Woellhaf, M. W., Herrmann, J. M., and Förster, F. (2015) Organization of the mitochondrial translation machinery studied *in situ* by cryoelectron tomography. *Nat. Commun.* **6,** 6019 CrossRef Medline
41. Bode, M., Woellhaf, M. W., Bohnert, M., van der Laan, M., Sommer, F., Jung, M., Zimmermann, R., Schroda, M., and Herrmann, J. M. (2015) Redox-regulated dynamic interplay between Cox19 and the copper-binding protein Cox11 in the intermembrane space of mitochondria facilitates biogenesis of cytochrome c oxidase. *Mol. Biol. Cell* **26,** 2385–2401 CrossRef Medline
42. Demishtein-Zohary, K., Günsel, U., Marom, M., Banerjee, R., Neupert, W., Azem, A., and Mokranjac, D. (2017) Role of Tim17 in coupling the import motor to the translocation channel of the mitochondrial presequence translocase. *eLife* **6,** e22696 CrossRef
43. Matta, S. K., Pareek, G., Bankapalli, K., Oblesha, A., and D'Silva, P. (2017) Role of Tim17 transmembrane regions in regulating the architecture of presequence translocase and mitochondrial DNA stability. *Mol. Cell Biol.* **37,** CrossRef Medline
44. Chacinska, A., Lind, M., Frazier, A. E., Dudek, J., Meisinger, C., Geissler, A., Sickmann, A., Meyer, H. E., Truscott, K. N., Guiard, B., Pfanner, N., and Rehling, P. (2005) Mitochondrial presequence translocase: switching between TOM tethering and motor recruitment involves Tim21 and Tim17. *Cell* **120,** 817–829 CrossRef Medline
45. Chacinska, A., Pfannschmidt, S., Wiedemann, N., Kozjak, V., Sanjuán Szklarz, L. K., Schulze-Specking, A., Truscott, K. N., Guiard, B., Meisinger, C., and Pfanner, N. (2004) Essential role of Mia40 in import and assembly of mitochondrial intermembrane space proteins. *EMBO J.* **23,** 3735–3746 CrossRef Medline
46. Xie, Y., and Varshavsky, A. (2001) RPN4 is a ligand, substrate, and transcriptional regulator of the 26S proteasome: a negative feedback circuit. *Proc. Natl. Acad. Sci. U. S. A.* **98,** 3056–3061 CrossRef Medline
47. Owsianik, G., Balzi L, L., and Ghislain, M. (2002) Control of 26S proteasome expression by transcription factors regulating multidrug resistance in *Saccharomyces cerevisiae*. *Mol. Microbiol.* **43,** 1295–1308 CrossRef Medline
48. Hahn, J. S., Neef, D. W., and Thiele, D. J. (2006) A stress regulatory network for co-ordinated activation of proteasome expression mediated by yeast heat shock transcription factor. *Mol. Microbiol.* **60,** 240–251 CrossRef Medline
49. Schmidt, R. M., Schessner, J. P., Borner, G. H., and Schuck, S. (2019) The proteasome biogenesis regulator Rpn4 cooperates with the unfolded protein response to promote ER stress resistance. *eLife* **8,** e43244 CrossRef
50. Kowalski, L., Bragoszewski, P., Khmelinskii, A., Glow, E., Knop, M., and Chacinska, A. (2018) Determinants of the cytosolic turnover of mitochondrial intermembrane space proteins. *BMC Biol.* **16,** 66 CrossRef Medline
51. Fischer, M., Horn, S., Belkacemi, A., Kojer, K., Petrungaro, C., Habich, M., Ali, M., Küttner, V., Bien, M., Kauff, F., Dengjel, J., Herrmann, J. M., and Riemer, J. (2013) Protein import and oxidative folding in the mitochondrial intermembrane space of intact mammalian cells. *Mol. Biol. Cell* **24,** 2160–2170 CrossRef Medline
52. Mohanraj, K., Wasilewski, M., Benincá, C., Cysewski, D., Poznanski, J., Sakowska, P., Bugajska, Z., Deckers, M., Dennerlein, S., Fernandez-Vizarra, E., Rehling, P., Dadlez, M., Zeviani, M., and Chacinska, A. (2019) Inhibition of proteasome rescues a pathogenic variant of respiratory chain assembly factor COA7. *EMBO Mol. Med.* **11,** e9561 CrossRef
53. Bragoszewski, P., Gornicka, A., Sztolsztener, M. E., and Chacinska, A. (2013) The ubiquitin-proteasome system regulates mitochondrial intermembrane space proteins. *Mol. Cell Biol.* **33,** 2136–2148 CrossRef Medline
54. Bragoszewski, P., Wasilewski, M., Sakowska, P., Gornicka, A., Böttinger, L., Qiu, J., Wiedemann, N., and Chacinska, A. (2015) Retro-translocation of mitochondrial intermembrane space proteins. *Proc Natl Acad Sci U S A* **112,** 7713–7718 CrossRef Medline
55. Morgenstern, M., Stiller, S. B., Lübbert, P., Peikert, C. D., Dannenmaier, S., Drepper, F., Weill, U., Höß, P., Feuerstein, R., Gebert, M., Bohnert, M., van der Laan, M., Schuldiner, M., Schütze, C., Oeljeklaus, S., *et al.* (2017) Definition of a high-confidence mitochondrial proteome at quantitative scale. *Cell Rep.* **19,** 2836–2852 CrossRef Medline
56. Thul, P. J., Åkesson, L., Wiking, M., Mahdessian, D., Geladaki, A., Ait Blal, H., Alm, T., Asplund, A., Björk, L., Breckels, L. M., Bäckström, A., Danielsson, F., Fagerberg, L., Fall, J., Gatto, L., *et al.* (2017) A subcellular map of the human proteome. *Science* **356,** eaal3321 CrossRef
57. Floyd, B. J., Wilkerson, E. M., Veling, M. T., Minogue, C. E., Xia, C., Beebe, E. T., Wrobel, R. L., Cho, H., Kremer, L. S., Alston, C. L., Gromek, K. A., Dolan, B. K., Ulbrich, A., Stefely, J. A., Bohl, S. L., *et al.* (2016) Mitochondrial protein interaction mapping identifies regulators of respiratory chain function. *Mol. Cell* **63,** 621–632 CrossRef Medline
58. Liu, X., Salokas, K., Tamene, F., Jiu, Y., Weldatsadik, R. G., Öhman, T., and Varjosalo, M. (2018) An AP-MS- and BioID-compatible MAC-tag enables comprehensive mapping of protein interactions and subcellular localizations. *Nat. Commun.* **9,** 1188 CrossRef Medline
59. Kunitomi, H., Kobayashi, Y., Wu, R. C., Takeda, T., Tominaga, E., Banno, K., and Aoki, D. (2020) LAMC1 is a prognostic factor and a potential therapeutic target in endometrial cancer. *J. Gynecol. Oncol.* **31,** e11 CrossRef Medline
60. Uhlen, M., Zhang, C., Lee, S., Sjöstedt, E., Fagerberg, L., Bidkhori, G., Benfeitas, R., Arif, M., Liu, Z., Edfors, F., Sanli, K., von Feilitzen, K., Oksvold, P., Lundberg, E., Hober, S., *et al.* (2017) A pathology atlas of the human cancer transcriptome. *Science* **357,** eaan2507 CrossRef Medline
61. Von Ohlen, T., Luce-Fedrow, A., Ortega, M. T., Ganta, R. R., and Chapes, S. K. (2012) Identification of critical host mitochondrion-associated genes during *Ehrlichia chaffeensis* infections. *Infect. Immun.* **80,** 3576–3586 CrossRef Medline
62. Su, A. I., Cooke, M. P., Ching, K. A., Hakak, Y., Walker, J. R., Wiltshire, T., Orth, A. P., Vega, R. G., Sapinoso, L. M., Moqrich, A., Patapoutian, A., Hampton, G. M., Schultz, P. G., and Hogenesch, J. B. (2002) Large-scale analysis of the human and mouse transcriptomes. *Proc. Natl. Acad. Sci. U. S. A.* **99,** 4465–4470 CrossRef Medline
63. Uhlén, M., Fagerberg, L., Hallström, B. M., Lindskog, C., Oksvold, P., Mardinoglu, A., Sivertsson, A., Kampf, C., Sjöstedt, E., Asplund, A., Olsson, I., Edlund, K., Lundberg, E., Navani, S., Szigyarto, C. A., *et al.* (2015) Proteomics. Tissue-based map of the human proteome. *Science* **347,** 1260419 CrossRef Medline
64. Bilodeau, M., MacRae, T., Gaboury, L., Laverdure, J. P., Hardy, M. P., Mayotte, N., Paradis, V., Harton, S., Perreault, C., and Sauvageau, G. (2009) Analysis of blood stem cell activity and cystatin gene expression in

a mouse model presenting a chromosomal deletion encompassing Csta and Stfa2l1. *PLoS ONE* **4,** e7500 CrossRef Medline

65. Hibbs, M. A., Hess, D. C., Myers, C. L., Huttenhower, C., Li, K., and Troyanskaya, O. G. (2007) Exploring the functional landscape of gene expression: directed search of large microarray compendia. *Bioinformatics* **23,** 2692–2699 CrossRef Medline
66. Shirozu, R., Yashiroda, H., and Murata, S. (2016) Proteasome impairment induces recovery of mitochondrial membrane potential and an alternative pathway of mitochondrial fusion. *Mol. Cell Biol.* **36,** 347–362 CrossRef Medline
67. Metzger, M. B., and Michaelis, S. (2009) Analysis of quality control substrates in distinct cellular compartments reveals a unique role for Rpn4p in tolerating misfolded membrane proteins. *Mol. Biol. Cell* **20,** 1006–1019 CrossRef Medline
68. Gebert, M., Schrempp, S. G., Mehnert, C. S., Heiëwolf, A. K., Oeljeklaus, S., Ieva, R., Bohnert, M., von der Malsburg, K., Wiese, S., Kleinschroth, T., Hunte, C., Meyer, H. E., Haferkamp, I., Guiard, B., Warscheid, B., *et al.* (2012) Mgr2 promotes coupling of the mitochondrial presequence translocase to partner complexes. *J. Cell Biol.* **197,** 595–604 CrossRef Medline
69. Mick, D. U., Dennerlein, S., Wiese, H., Reinhold, R., Pacheu-Grau, D., Lorenzi, I., Sasarman, F., Weraarpachai, W., Shoubridge, E. A., Warscheid, B., and Rehling, P. (2012) MITRAC links mitochondrial protein translocation to respiratory-chain assembly and translational regulation. *Cell* **151,** 1528–1541 CrossRef Medline
70. Janke, C., Magiera, M. M., Rathfelder, N., Taxis, C., Reber, S., Maekawa, H., Moreno-Borchart, A., Doenges, G., Schwob, E., Schiebel, E., and Knop, M. (2004) A versatile toolbox for PCR-based tagging of yeast genes: new fluorescent proteins, more markers and promoter substitution cassettes. *Yeast* **21,** 947–962 CrossRef Medline
71. Livak, K. J., and Schmittgen, T. D. (2001) Analysis of relative gene expression data using real-time quantitative PCR and the $2^{-\Delta\Delta CT}$ Method. *Methods* **25,** 402–408 CrossRef Medline
72. Teste, M. A., Duquenne, M., François, J. M., and Parrou, J. L. (2009) Validation of reference genes for quantitative expression analysis by real-time RT-PCR in *Saccharomyces cerevisiae*. *BMC Mol. Biol.* **10,** 99 CrossRef Medline
73. Eden, E., Navon, R., Steinfeld, I., Lipson, D., and Yakhini, Z. (2009) GOrilla: a tool for discovery and visualization of enriched GO terms in ranked gene lists. *BMC Bioinformatics* **10,** 48 CrossRef Medline